Human Molecular Genetics, 2013, Vol. 22, No. 11 **2129–2140**
doi:10.1093/hmg/ddt061
Advance Access published on February 7, 2013

Dopaminergic expression of the Parkinsonian gene *LRRK2-G2019S* leads to non-autonomous visual neurodegeneration, accelerated by increased neural demands for energy

Samantha Hindle†, Farinaz Afsari, Meg Stark, C. Adam Middleton, Gareth J.O. Evans, Sean T. Sweeney and Christopher J.H. Elliott*

Department of Biology, University of York, York YO10 5DD, UK

Received December 20, 2012; Revised and Accepted February 5, 2013

Parkinson's disease (PD) is associated with loss of dopaminergic signalling, and affects not just movement, but also vision. As both mammalian and fly visual systems contain dopaminergic neurons, we investigated the effect of LRRK2 mutations (the most common cause of inherited PD) on Drosophila electroretinograms (ERGs). We reveal progressive loss of photoreceptor function in flies expressing *LRRK2-G2019S* in dopaminergic neurons. The photoreceptors showed elevated autophagy, apoptosis and mitochondrial disorganization. Head sections confirmed extensive neurodegeneration throughout the visual system, including regions not directly innervated by dopaminergic neurons. Other PD-related mutations did not affect photoreceptor function, and no loss of vision was seen with kinase-dead transgenics. Manipulations of the level of *Drosophila* dLRRK suggest *G2019S* is acting as a gain-of-function, rather than dominant negative mutation. Increasing activity of the visual system, or of just the dopaminergic neurons, accelerated the *G2019S*-induced deterioration of vision. The fly visual system provides an excellent, tractable model of a non-autonomous deficit reminiscent of that seen in PD, and suggests that increased energy demand may contribute to the mechanism by which *LRRK2-G2019S* causes neurodegeneration.

INTRODUCTION

Parkinson's disease (PD), characterized by a loss of dopaminergic neurons, is generally described as a movement disorder. However, patients also experience a range of other symptoms, including cognitive changes (e.g. mood, dementia) and visual problems (from dry eyes and difficulties with reading, to hallucinations and perceptual disorders) (1). Some of these symptoms may be due to difficulties in the coordination and contraction of the eye muscles, but other symptoms may arise from deficits in signalling in the visual system as a result of dopaminergic neuron loss. Tyrosine-hydroxylase (TH) staining in the human retina identifies the A18 amacrine cells as dopaminergic (2). A18 neurons have major roles in the processing of edges and outlines (crucial to shape discrimination), in light adaptation and in diurnal rhythms (3,4). These neurons have decreased levels of dopamine in PD patients (5), possibly explaining the physiological deficits in retinal signalling in these patients (6).

Like mammals, insects have dopaminergic neurons with axons branching in the visual system (7–9) (see also Fig. 7A). Other similarities between insects and mammals lie in the functions suggested for dopamine in the retina: adaptation to bright lights (10) and diurnal rhythms (11,12). Thus homology not only exists between fly and human in the PD-related fields of genetics and cell biology, but also in the organization of the visual system. Advantageously, the anatomy of the fly eye makes it straightforward to record the electroretinogram (ERG, Fig. 1A), while fly genetics provides the experimental selectivity of the GAL4-UAS system to analyse the effects of expressing PD-related genes carrying associated mutations. Here we focus on the dominant

*To whom correspondence should be addressed. Tel: +44 1904 328654; Fax: +44 1904 328505; Email: cje2@york.ac.uk
†Present address: Department of Anesthesia, University of California San Francisco, Genentech Hall, 600 16th Street, San Francisco, CA, USA.

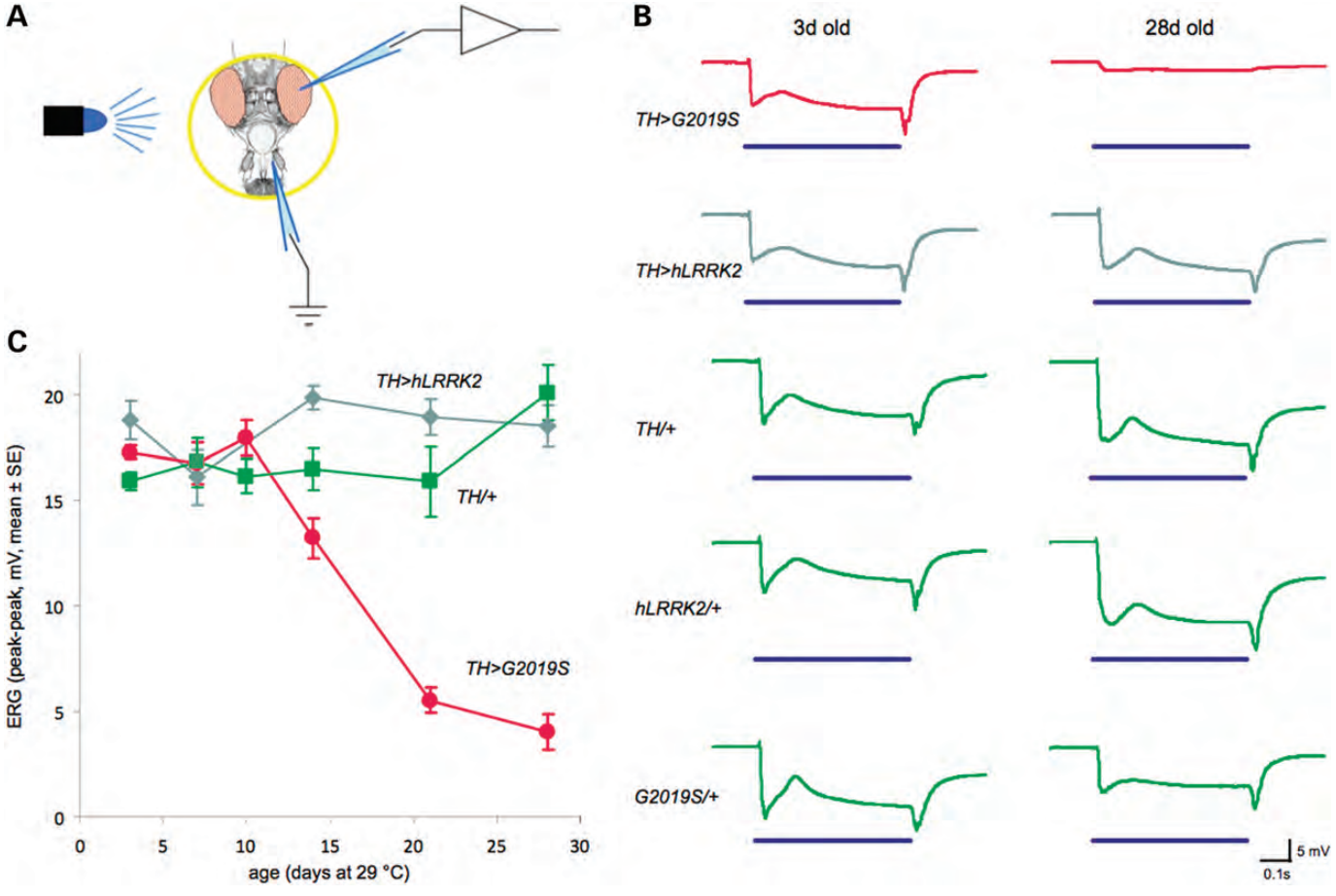

Figure 1. Expressing the *G2019S* mutation of *LRRK2* in the dopaminergic neurons causes a rapid decline in visual function. (**A**) Visual function is assessed by electroretinograms (ERGs), in which an electrical recording is made from the surface of the eye, with a reference electrode in the mouthparts. The response to 500 ms pulse of blue light is recorded. (**B**) A sample recording from a fly with *G2019S* expressed in the dopaminergic neurons using the tyrosine hydroxylase (TH) GAL4 driver (*TH > G2019S*, red trace), shows a normal ERG at 3 days, but a minimal response by 28 days. Flies expressing wild-type *hLRRK2* and control outcrosses (green) show normal ERGs at both 3 and 28 days. (**C**) The decline in visual function with *TH > G2019S* begins at 10 days and drops steeply thereafter, but flies expressing *hLRRK2* or control outcross (*TH/+*) maintain constant visual function. Analysis of 178 flies (8–13 flies of each genotype at each timepoint, see Supplementary Material, Table S1), kept dark in a 29°C incubator.

G2019S mutation in *LRRK2* kinase, as this mutation is the most common cause of inherited late-onset PD.

RESULTS

Our key result is that expressing the *LRRK2-G2019S* mutation in just the dopaminergic neurons leads to loss of ERG response between 10 and 28 days, with the peak–peak amplitude dropping from 17 ± 0.3 to 4 ± 0.8 mV (mean $\pm$ SE) (Fig. 1B and C and 2B†). All components of the ERG (the on-transient, maintained response and off-transient) are reduced by 28 days (Supplementary Material, Fig. S1). As the response becomes smaller, the return to baseline surprisingly takes longer ($t_{\frac{1}{2}}$ increases 5-fold). We observed a similar loss of visual response in a second, independently generated *G2019S* line (13) when driven with the *TH* GAL4 (Fig. 2B*). No loss of response is seen when the normal wild-type *hLRRK2* gene is expressed in dopaminergic neurons (Fig. 1B and C, Fig. 2B, two independent strains * and †), even though hLRRK2 may be expressed at a slightly higher level (Supplementary Material, Fig. S2B) (14). Normal ERGs were also recorded when expression of the fly homologue *dLRRK* is increased (Fig. 2B, left-hand bar) or in control outcrosses (Fig. 2C, right-hand bars; Supplementary Material, Fig. S3).

In order to investigate the selectivity of the decline in visual function for *G2019S*, we expressed transgenes bearing seven further single amino-acid mutations in the dopaminergic neurons of the fly brain, all using the same driver (*TH* GAL4). These mutations are all at sites known to be pathogenic or to segregate with PD, and were encoded either in the human *UAS-hLRRK2* sequence or the fly *UAS-dLRRK* sequence (Fig. 2A). None of the other transgenes showed a significant reduction in ERG amplitude by 28 days (Fig. 2B), showing this phenotype is highly sensitive to the *G2019S* mutation. Western blots suggested that expression of the other FLAG-tagged *LRRK2* transgenes was at a comparable (or greater) level than *G2019S* (Supplementary Material, Fig. 2A and B).

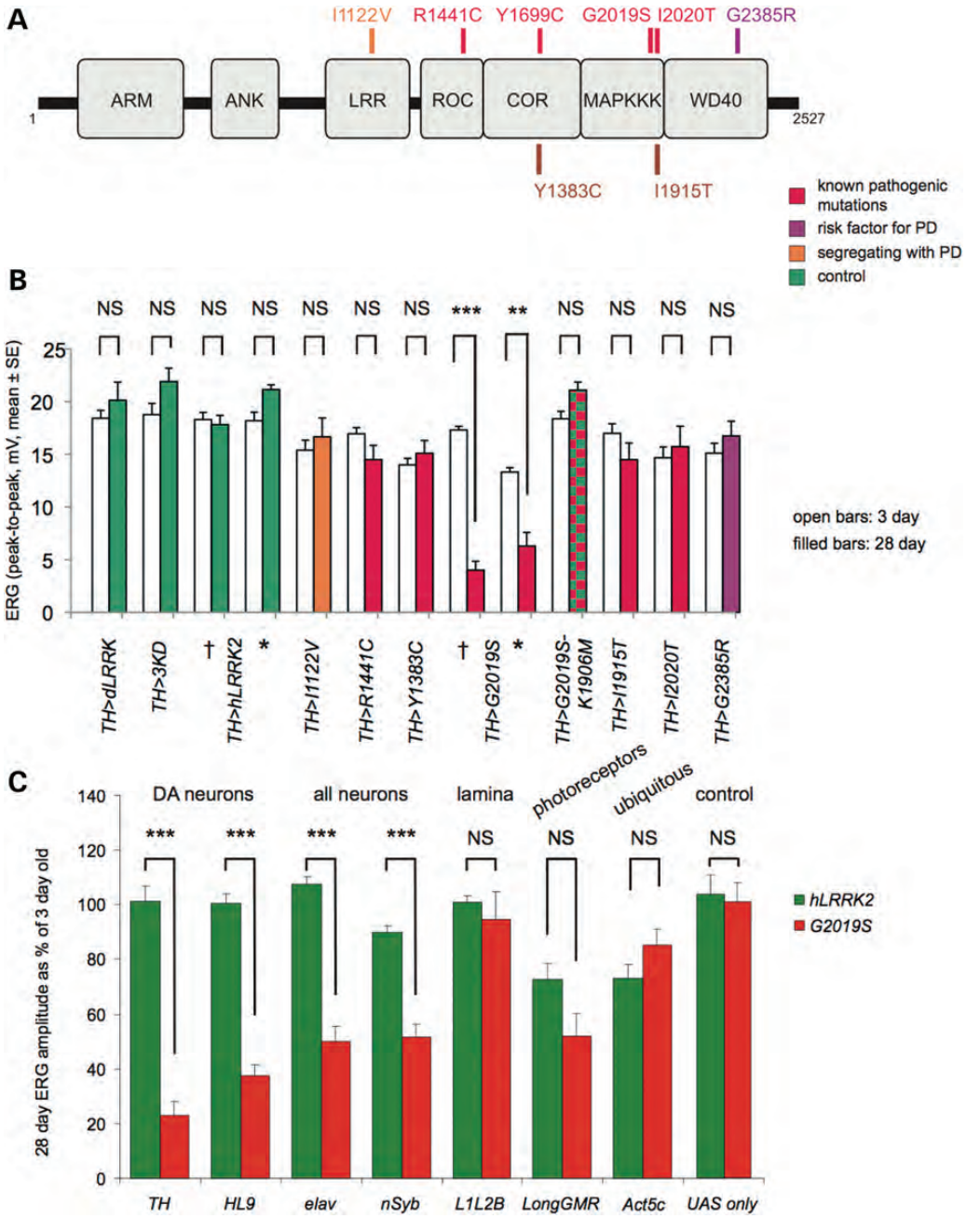

Figure 2. Visual degeneration is specific for expression of the *G2019S* mutation in dopaminergic neurons. (**A**) Location of the LRRK2 mutations used in this study, on a scale diagram of the protein domains [(modified after Kumari and Tan (54)]. The position and pathological status of each mutation (orange/red/purple) is shown above the domain diagram. (**B**) Expression of these *LRRK2* mutations with the *TH* GAL4 shows that only the *G2019S* mutation leads to a significant reduction in electroretinogram (ERG) amplitude at 28 days. No effect was seen with the expression of *hLRRK2*. This difference was seen in two independently generated lines [† (14), all the other data in this paper are derived from these lines; * (13)]. We found similar levels of expression of *LRRK2* transgenics derived from different labs (Supplementary Material, Fig. S2), so that the differences in ERGs cannot be ascribed to differences in expression levels. No decline in visual response is seen with kinase dead mutations (*dLRRK-3KD* and *G2019S-K1906M*), or with those in the GTP-binding domain (e.g. *R1441C*). The *Y1383C* and *I1915T* mutations are expressed in the fly LRRK sequence. (**C**) The loss of visual function at 28 days is most severe when *G2019S* is driven with *TH* or *HL9* GAL4 which only express in the dopaminergic neurons. Expression of *G2019S* in all neurons using either the *elav* or *nSyb* GAL4 drivers gives a significant reduction in the ERG amplitude, but it is not as severe as when *G2019S* is only expressed in the dopaminergic neurons. There is no decline in ERG amplitude when *G2019S* is expressed with the *L1L2B* GAL4, into the second order lamina neurons. Although the mean ERG response appears less when *G2019S* is expressed with the ubiquitous (*Act5c*) or with the photoreceptor-specific (*LongGMR*) GAL4, this was not significant (Bonferroni $P = 1.0$ and 0.11, respectively). In all these cases, expressing the normal *hLRRK2* gave no significant loss of visual function over 28 days. Neither UAS-control showed any decline in visual function. Data from 295 flies for (B) and 360 for (C), at least eight flies of each genotype at a timepoint (see Supplementary Material, Table S1). Bonferroni *post-hoc* test, $^{**}P < 0.01$; $^{***}P < 0.001$; all flies were kept in the dark incubator.

We took advantage of the range of highly specific GAL4 drivers to identify the susceptibility of fly tissues to the *LRRK2-G2019S* mutation (Fig. 2C). With both the *TH* GAL4 and a second dopaminergic neuron driver (*HL9* GAL4), we observed a severe loss of visual function at 28 days with *G2019S* expression (down to 23 and 37%, respectively), but expressing *hLRRK2* did not affect visual function by 28 days (ANOVA, Bonferroni comparison of *G2019S* and *hLRRK2* expression: $P < 0.001$ for both GAL4 drivers). We then used two different GAL4 lines (*elav* and *nSyb*), both specific for broad neuronal expression. In both conditions, we found a ~50% loss of ERG amplitude at 28 days when *G2019S* was expressed, but no loss of response with *hLRRK2* (ANOVA, Bonferroni $P < 0.001$ for both *elav* and *nSyb*). We next expressed these *LRRK2* transgenes in the lamina neurons (second-order neurons which make synaptic contact with the photoreceptors) using the *L1L2B* GAL4 (15). Here we found no change over 28 days in the peak–peak amplitude of the ERG with either *LRRK2* transgene. When *LRRK2-G2019S* is expressed in just the photoreceptors (*LongGMR* GAL4), or ubiquitously (*Actin5C* GAL4) the ERG amplitude declines over 28 days, but there is no significant difference between expression of *G2019S* or *hLRRK2*. In control experiments (four different GAL4/wild-type outcrosses, one wild-type outcross, and with two UAS/ wild-type outcrosses), we found no significant change in ERG amplitude (Fig. 2C, Supplementary Material, Fig. S3).

Our data—that the decline in visual response is specific for the *G2019S* mutation—is in accordance with the hypothesis that the key function of LRRK2 (at least in the visual system) is as a kinase. We tested this hypothesis by expressing the *LRRK2-G2019S-K1906M* transgene, in which kinase activity has been abolished by the K1906M amino-acid substitution in the (presumed) ATP-binding site. We found no loss of ERG response in the *TH > LRRK2-G2019S-K1906M* flies, as would be expected if the kinase is the key function of *LRRK2* in the visual system. Western blots suggest that the *G2019S* and *G2019S-K1906M* proteins are expressed at similar levels (Fig. 2A), so the difference does not seem to be due to a failure of protein production.

It has been suggested (16,17) that *G2019S* may be a simple gain-of-function (GOF) mutation, increasing the rate of phosphorylation of LRRK2 substrates, or it might act as a dominant negative (DN). If *G2019S* were a DN mutation, we would expect the effect of *G2019S* expression to be stronger when the amount of the flies' own dLRRK is reduced. We directly tested this by putting *TH > G2019S* in a *dLRRK̄* heterozygote background. Our data do not support the DN hypothesis: *G2019S* was much less effective at reducing the amplitude of the ERG in the *dLRRK̄* heterozygote background (Fig. 3). Our data rather accords with the hypothesis that the *G2019S* is a simple GOF mutation.

We next asked if the functional decline in vision is accompanied by anatomical evidence of neurodegeneration. We found that, after 28 days, the *TH > G2019S* flies showed strong neurodegeneration throughout the internal structure of the retina, which became disorganized, while the visual lobes (lamina and medulla) showed frequent vacuoles (Fig. 4A). No such features were seen in *TH > hLRRK2* flies or in wild-type controls. This was accompanied by evidence of increased

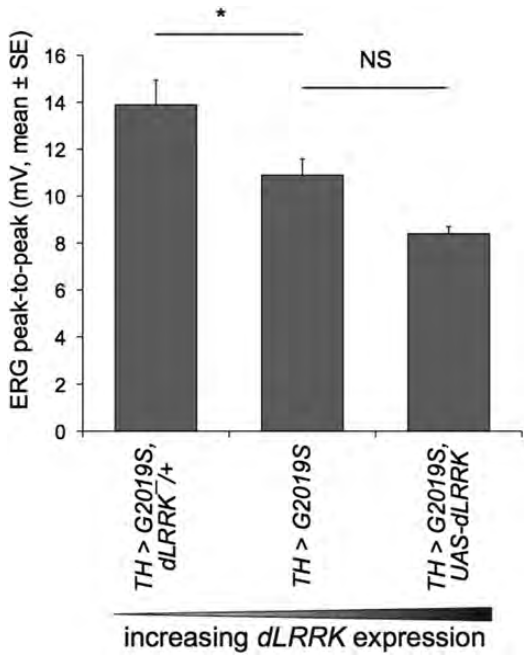

Figure 3. Loss of the electroretinogram (ERG) response due to *TH > G2019S* is reduced by decreasing expression of *Drosophila* LRRK (dLRRK). *G2019S* was expressed by *TH* GAL4 either in a background in which one copy of the *dLRRK* gene was knocked out (*dLRRK̄*/+), or in the wild-type background, or in flies in which *dLRRK* was overexpressed by the *TH* GAL4 driver. Data from 35 flies (3 days old, 11 from each genotype, see Supplementary Material, Table S1) kept at 29°C in tubes where the blue light was turned on/off at 1 s intervals. Bonferroni *post-hoc* test, $^*P < 0.05$

autophagy and apoptosis around the microvilli of the photoreceptors in 21–23-day-old *TH > G2019S* flies (Fig. 5). Additionally, the photoreceptor mitochondria become swollen (70% increase in area), and the cristae wider (80% wider) and become more broken, fragmented and rounded (Fig. 6). Although the internal structure of the *TH > G2019S* retina is degenerating, the exterior surface of the eyes of all 28-day-old flies was normal in all our experiments. We observed none of the developmental abnormalities (irregular ommatidia or black pigmentation) reported in flies raised at 29°C (18). This included our *TH > G2019S* and *TH > hLRRK2* crosses (Fig. 4B) and the flies expressing *G2019S* or *hLRRK2* with the *Act5C, LongGMR* and *elav* GAL4 drivers (Supplementary Material, Fig. S4).

A second anatomical question is whether the loss of visual response and degeneration of the photoreceptor layer is preceded by (or correlated with) a loss of dopaminergic innervation of the visual lobes. As dopaminergic transgenics and antibodies have been reported to highlight different groups of neurons (19), we used three GFP reporters under the control of two different dopaminergic GAL4 drivers and compared this with staining by tyrosine hydroxylase antibody (α-TH). In young control flies, we found three kinds of innervation of the visual lobes. First, the PPL neurons, which branch densely in the innermost visual neuropil (the lobula), which are α-TH positive and which express all the GFPs tested with *TH* GAL4 (Fig. 7B and C). We did not see the PPL neurons whenever the *HL9* GAL4 was used. Secondly, the abundant MC neurons (Fig. 7B and C), with their cell

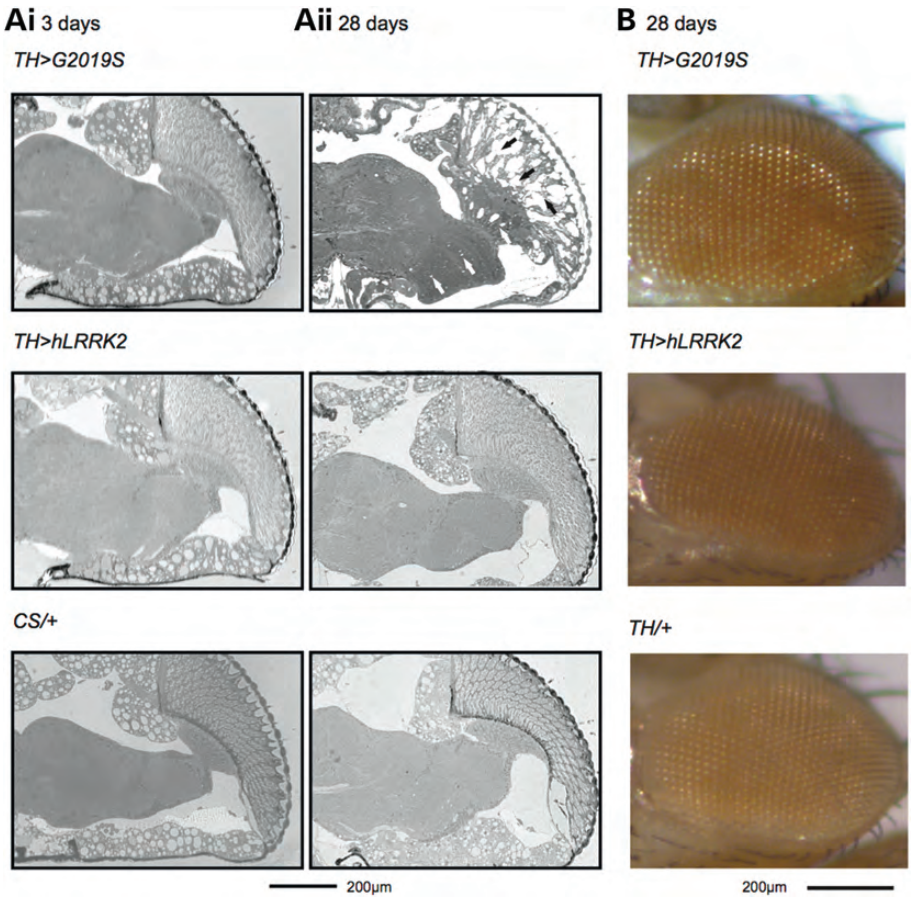

Figure 4. Loss of visual function with *G2019S* is accompanied by anatomical degeneration. (**A**) Sections of the head of a 28-day-old *TH > G2019S* fly shows extensive degeneration (ii), with many vacuoles in the retina, lamina and lobula, but there is no degeneration in the 3-day-old fly (i), or in a *TH > hLRRK2* or control (*CS*/+) fly of the same age. (Sections representative of three flies of each genotype.) (**B**) No external defects are seen in the eyes of flies expressing *G2019S* or *hLRRK2* in the dopaminergic neurons (*TH > G2019S, TH > hLRRK2*, respectively), and of a control (*TH*/+) fly shown at 28 days. In all panels, anterior is to the top. In the eye surface images, dorsal is to the right. All flies were kept dark in the incubator.

bodies at the edge of the medulla and axons projecting radially in towards the core of the medulla, stained reliably with α-TH. As expected (8), only a proportion of the MC neurons are reported by any GFP. Thirdly, we observed a cluster of approximately four neurons projecting from the lateral edge of the protocerebrum, across the anterior face of the medulla to the lamina. As these neurons have not previously been reported, we have labelled them as LA neurons as they branched extensively and gave rise to blebs in the lamina, suggesting synaptic release sites. These neurons were reliably seen both with *TH >* GFP (Fig. 7D) and *HL9 >* GFP (Fig. 7E), but were not seen with α-TH. We also observed each of these three types of neurons in young flies expressing either *G2019S* or *hLRRK2* with *TH* GAL4 (data not shown). In the 28-day-old *TH > G2019S* flies, all three types of neurons are still present, and we did not see any reduction in the number of cell bodies or axonal branching (Fig. 8). We specifically used the eIf-4A3-GFP reporter in these experiments, as it has a strong nuclear fluorescence, but we did not see any sign of damage to the cell bodies. All these neurons were also present in the 28-day-old *TH > hLRRK2* and control flies (data not shown).

In search of a mechanism for loss of visual response, we tested if physiological and neurodegenerative decline is driven by activity (or energy) demand. We addressed this in two experiments, first by keeping flies in irregularly pulsating light, so that the visual system continually has to adapt to new light levels, and second by increasing the activity of the dopaminergic neurons genetically. If these treatments were to accelerate visual neurodegeneration, we might expect to see a loss of ERG amplitude sooner than normal; therefore we tested these flies at 10 days, a time before any loss of visual response is normally seen in the *TH > G2019S* flies (Fig. 1C).

In our first experiment, we kept flies in constant dark, constant light, and in vials where the light was pulsed on and off randomly at ∼1.5 s intervals. When we tested 10-day-old flies, we first found that those kept in constant light were less sensitive to our test stimulus than flies kept in the dark (Fig. 9A). This is as expected: flies have long-term adaptations to constant light. Importantly, there was no difference between *TH > hLRRK2* and *G2019S* lines in either constant dark or constant light. However, the *G2019S* flies kept in pulsating light showed reduced ERG response to the test stimulus compared with the *hLRRK2* flies, or with their counterparts in constant light. No such decrement is seen in the *hLRRK2* flies.

In our second experiment, we manipulated the electrical activity of the dopaminergic neurons. We took advantage of the

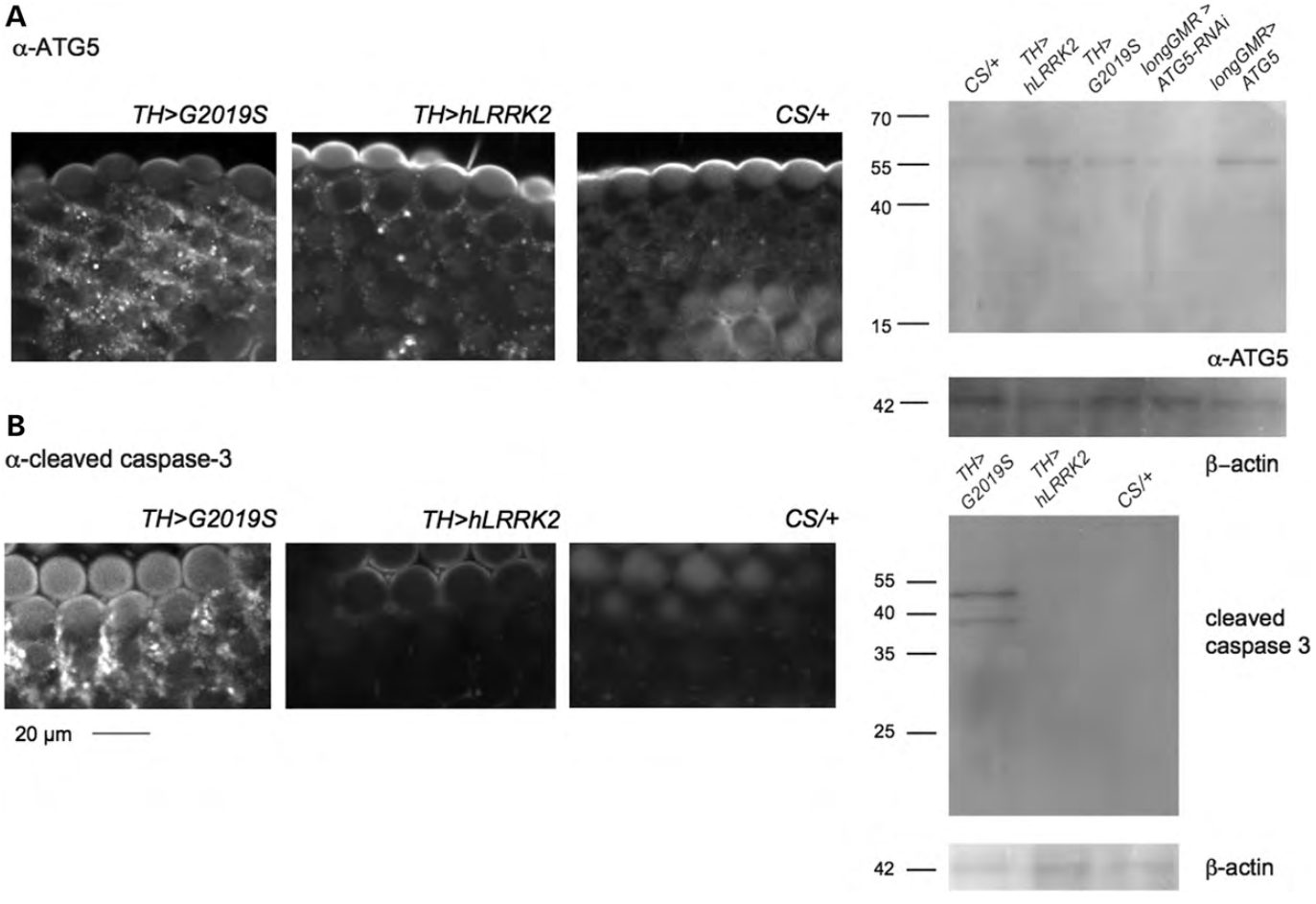

Figure 5. Autophagy and apoptosis are increased in the outer part of the photoreceptor layer in 22-day-old *TH > G2019S* flies. Grazing sections of the eyes of *TH > G2019S*, *TH > hLRRK2* and control (*CS/+*) flies. (**A**) Upregulation of the autophagy gene ATG5 in the *TH > G2019S* micrograph in the photoreceptors (at the level of the microvilli) as shown by extensive fluorescence around the edges of the ommatidia; the *TH > hLRRK2* micrograph shows occasional puncta and the wild-type outcross (*CS/+*) is nearly free of staining. Western blots from the whole eye suggest autophagy is increased in both *TH > G2019S* and *TH > hLRRK2* flies compared with the wild-type control (*CS/+*). The two right-hand lanes show additional controls, with reduced intensity when ATG5 knocked down in the eye by *longGMR > ATG5-RNAi* and increased intensity when ATG5 expression is increased by *longGMR >* UAS-*ATG5*. (**B**) The cleaved caspase-3 antibody, used in flies as a marker of activity by the initiator caspase DRONC (52,53), is widely bound in *TH > G2019S*, but only present in small spots between the ommatidia in the *TH > hLRRK2* and control (*CS/+*). Western blots from the eyes of 23-day-old *TH > G2019S* flies show bands corresponding to the caspase-3-like effector caspases DRICE and DCP-1. There is no expression of apoptotic proteins in the *TH > hLRRK2* or CS/+ wild-type control.

electrical-knock-in (*EKI*) transgene, a combination of *shaker* (*sh)* and *ether a go-go* (*eag*) dominant negative constructs (20,21), which reduces potassium-channel function and so makes neurons (in which it is expressed) more active. At 3 days, all genotypes had normal vision (Fig. 9B). At 10 days, the *TH > G2019S* animals, *TH >* EKI animals and control out-cross animals all had the expected normal full visual response. However, flies expressing both the *G2019S* and *EKI* constructs in the dopaminergic neurons had already started to lose their visual function: they had significantly smaller ERGs (71%) than those expressing *G2019S* or *EKI* alone. Thus knockout of the *shaker* and *ether a go-go* channels in just the dopaminergic neurons increases their sensitivity to the *G2019S* form of *LRRK2*.

DISCUSSION

We have demonstrated functional and anatomical loss of visual response as a consequence of expressing the most common Parkinson's disease-related mutation (*LRRK2-G2019S*) selectively in the dopaminergic neurons. This is caused by progressive neuronal dysfunction rather than a developmental defect because young flies ($\leq$10 days old) have normal vision, the external structure of the eye is not compromised and the loss of visual response and anatomical disorganization occurs gradually. The loss of visual function is highly specific for the combination of the dopaminergic neurons with *LRRK2-G2019S* mutation. Of the mutations which we tested *in vivo*, in previous biochemical assays, only *G2019S* more than doubles the LRRK2 kinase activity with all the substrates tested (22). Some of the kinase assays suggested that the *G2019S* mutation may be acting in a dominant negative manner (16,17), but our data indicate a simpler, GOF effect of the *G2019S* mutation.

Physiologically, our light stimuli excite the photoreceptors, which in turn excite second-order lamina or medulla neurons. The loss of the maintained component of the ERG in *TH > G2019S* flies indicates failure of these primary photoreceptors

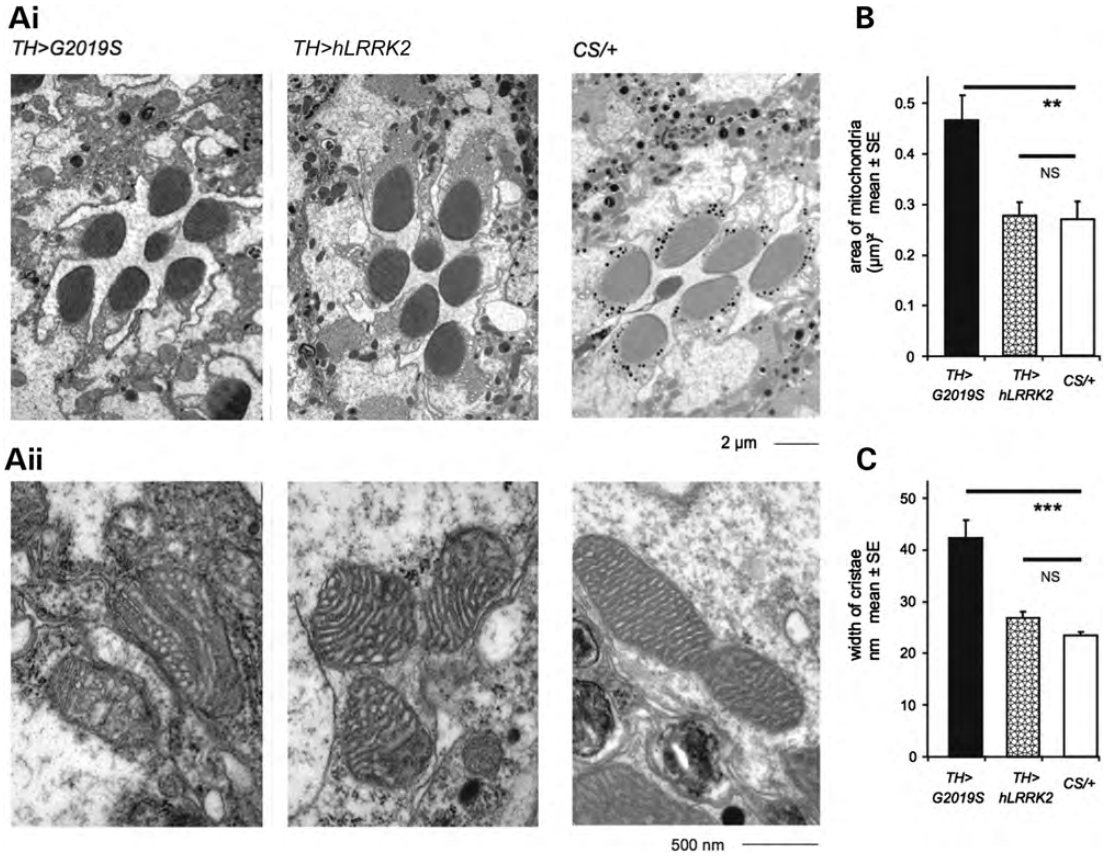

Figure 6. The photoreceptor mitochondria are dilated and have aberrant cristae in 28-day-old *TH > G2019S* flies. (**A**) Electron micrographs at the outer level of the microvilli from *TH > G2019S*, *TH > hLRRK2* and control (*CS*/+) flies. (Ai) Images centred on the ommatidium; the mitochondria are distributed around the edge of the ommatidia. (Aii) Higher magnification images, showing the enlarged mitochondria with dilated and disorganized cristae. (**B**) Quantification of the mitochondrial area. (**C**) Quantification of the width of the cristae. Summary data from 85 mitochondria in nine preparations. Bonferroni *post-hoc* tests, $^{**}P < 0.01$; $^{***}P < 0.001$.

to respond. The loss-of-function is accompanied by extensive anatomical changes, with both autophagy and apoptosis occurring around the photoreceptors. The photoreceptors also show evidence of mitochondrial failure. Anatomical evidence of degeneration of fly photoreceptors has been seen following expression of PD-related genes (*α-synuclein*, *parkin* and several *LRRK2* transgenes) in the eye using the *GMR* GAL4 (14,18,23,24), though this was not seen by all studies (25,26). Similarly, mitochondrial degeneration is seen in the fly flight muscle when *LRRK2-G2019S* is expressed using a muscle-specific driver (27). Degeneration and mitochondrial failure are key features of *LRRK2-G2019S* PD (28). While cell models indicate a loss of neuronal growth with *LRRK2-G2019S* (29), this is not the key finding of this report. However, we cannot exclude a moderate loss of the dopaminergic neurons, especially of the numerous MC cells. In all these previous papers, the degeneration is occurring in the tissue in which the *G2019S* transgene is expressed. Our data are different: we report a non-autonomous dysfunction and anatomical degeneration.

Thus, a crucial point here is that we are expressing the transgene in the dopaminergic neurons, but the physiological and anatomical loss we see is occurring elsewhere, in the photoreceptors and other regions of the visual system. What possible connections are there between the dopaminergic neurons in which *G2019S* is produced and the cells that die? Three kinds of dopaminergic neurons innervate the visual system: the PPL neurons in the lobula, the MC neurons in the medulla and the LA neurons which project from protocerebrum to the lamina. We may initially discount the PPL neurons because (i) they are not marked by the *HL9* GFP reporter (and *HL9 > G2019S* is as effective as *TH > G2019S* in causing loss of visual function) and (ii) these neurons only project to the lobula, well away from the photoreceptor terminals. We have no evidence that the MC neurons connect to the photoreceptors or laminal layers: the closest they approach is in the outer part of the medulla (7). While the axons of the ultraviolet sensitive R7 and R8 photoreceptors do terminate in the medulla (9), electron microscopy indicates there are no direct synapses between the MC dendrites and photoreceptor axons (30). The most likely type of dopaminergic neurons to interact with the photoreceptors is therefore the LA neurons: they are GFP-positive with both the *TH* and *HL9* GAL4 drivers, and their blebbed endings in the lamina allow us to speculate that they might release neurotransmitter near the photoreceptor terminals.

Nonetheless, whether there is synaptic contact or not, we are expressing *G2019S* in one class of cells, and recording functional and anatomical loss in a second kind of cell. Both

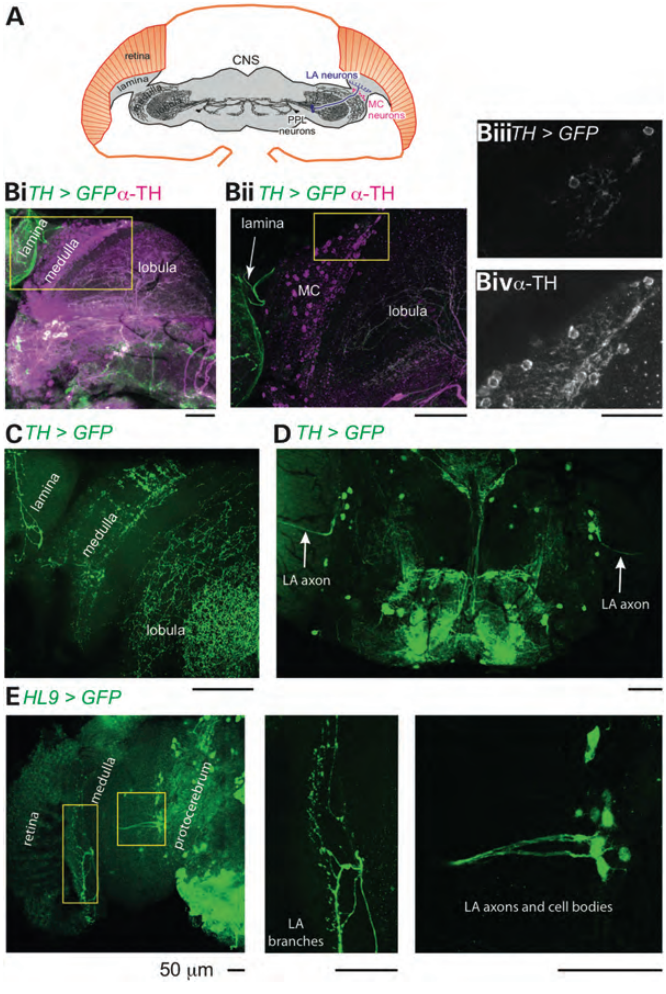

Figure 7. Dopaminergic neurons innervate three visual neuropiles, the lamina, medulla and lobula in 3-day-old flies. (**A**) Overview of the brain of the fly, showing the organization of the visual [optic] lobes. The visual neuropiles beneath the retina (the lamina, medulla and lobula complex) contain three kinds of dopaminergic neurons: the PPL neurons, the MC neurons and the LA neurons. The cell bodies of the PPL neurons reside in the central brain and send projections into the lobula. The cell bodies of the MC neurons are present on the surface of the medulla and send branches into the medulla neuropil. The LA neurons have cell bodies in the lateral protocerebrum with axons that run over the anterior face of the medulla and branch throughout the lamina (not previously described). (**Bi**) Low-power projection of a z-stack of brain and visual lobes, showing innervation of the lamina (GFP, green), the cell bodies and branches of the MC neurons in the medulla (α-TH, magenta) and intense TH staining in the lobula (PPL neurons, both α-TH, magenta; GFP, green). The yellow rectangle is shown magnified, in a thinner z-stack projection, to the right (Bii). Most MC cells were only marked with α-TH (Biii), but a few cells are also stained with GFP (Biv). (**C**) Confocal projection of the visual lobes, showing innervation of the lamina by the LA neurons, the MC cell bodies in the outer layer of the medulla and their axons projecting centrally, and the extensive branching of the PPL neurons in the lobula. (**D**) Low-power view of the complete central brain, showing the axons of the LA neurons on both left and right sides of the brain. (**E**) The LA neurons are also stained when GFP is expressed by the HL9 GAL4. The right panels show higher power views of the lamina branching and of the LA axons and cell bodies. Genotypes were: (B and C): *TH-GAL4 > UAS-myr-GFP*; (D): *TH-GAL4 > eIf-4A3-GFP*; E: HL9-GAL4 > *eIf-4A3-GFP*. Representative of 12 *TH* GAL4 and 12 *HL9* GAL4 preparations, oriented with lateral to the left.

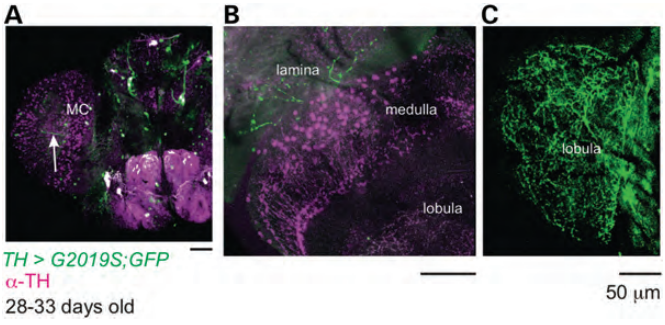

Figure 8. There is no loss of dopaminergic innervation of the optic lobes in 28–33-day-old *TH > G2019S* flies. (**A**) Overview of the brain, showing the MC neurons stained with anti-TH antiserum (α-TH, magenta) and the axons of the LA neurons (stained with GFP, green, arrow). (**B**) Higher power view of the visual lobes in another preparation, showing the LA axons branching in the lamina (GFP, green), the MC neurons and their branches in the outer medulla (α-TH, magenta) and the terminations of the PPL neurons in the lobula (both α-TH, magenta and GFP, green). (**C**) Micrograph of the lobula from a third preparation, showing the dense branching of the PPL neurons (GFP, green). All data are from preparations expressing both *G2019S* and *eIf-4A3-GFP* under the *TH*-GAL4. Representative of 18 preparations, oriented with lateral to the left.

physiological and anatomical criteria therefore indicate a spreading problem, with the loss of neuronal integrity occurring non-autonomously. Possible explanations of this include misregulation of dopamine (31) (or some co-transmitter), changes in the secretion of growth factors or diffusion of reactive oxygen species, or cell–cell transmission of mis-folded proteins (32).

Our data also show that increasing the demands on the visual system to adapt, or increasing the activity of just the dopaminergic neurons, accelerates the decline in visual function due to *G2019S* expression. After each action potential, the dopaminergic neurons are required to pump cations back across the plasma membrane. Such pumping requires energy from the mitochondria in the form of ATP. Ionic pumping already accounts for ~40% of the energy requirements of the CNS (33); the neurons of the fly visual system also have high demands for ATP (34). Thus, increase in neuronal activity is likely to couple harmfully with mitochondrial dysfunction, now accepted as a key feature of many forms of inherited PD. This could also lead to elevated or mis-regulated calcium flux, further exacerbating the situation. Increases in cation flux in fly photoreceptors or manipulations of mitochondrial ATP production in the fly retina cause rapid neurodegeneration (35–37). We recently reported a failure to maintain the normal resting potential at the *Drosophila* neuromuscular junction in the *parkin* knockout (38), while in mouse models of PINK1, HtrA2/Omi and DJ-1, hyperexcitability has also been reported (39,40). Our current data take this approach a step further, by showing that the progression of neurodegeneration (as monitored by loss of ERG response) can be affected by manipulation of the demand for energy.

Although fly models of inherited PD have generally reported a more consistent phenotype than mouse models, there are discrepancies in the fly data, e.g. in counts of

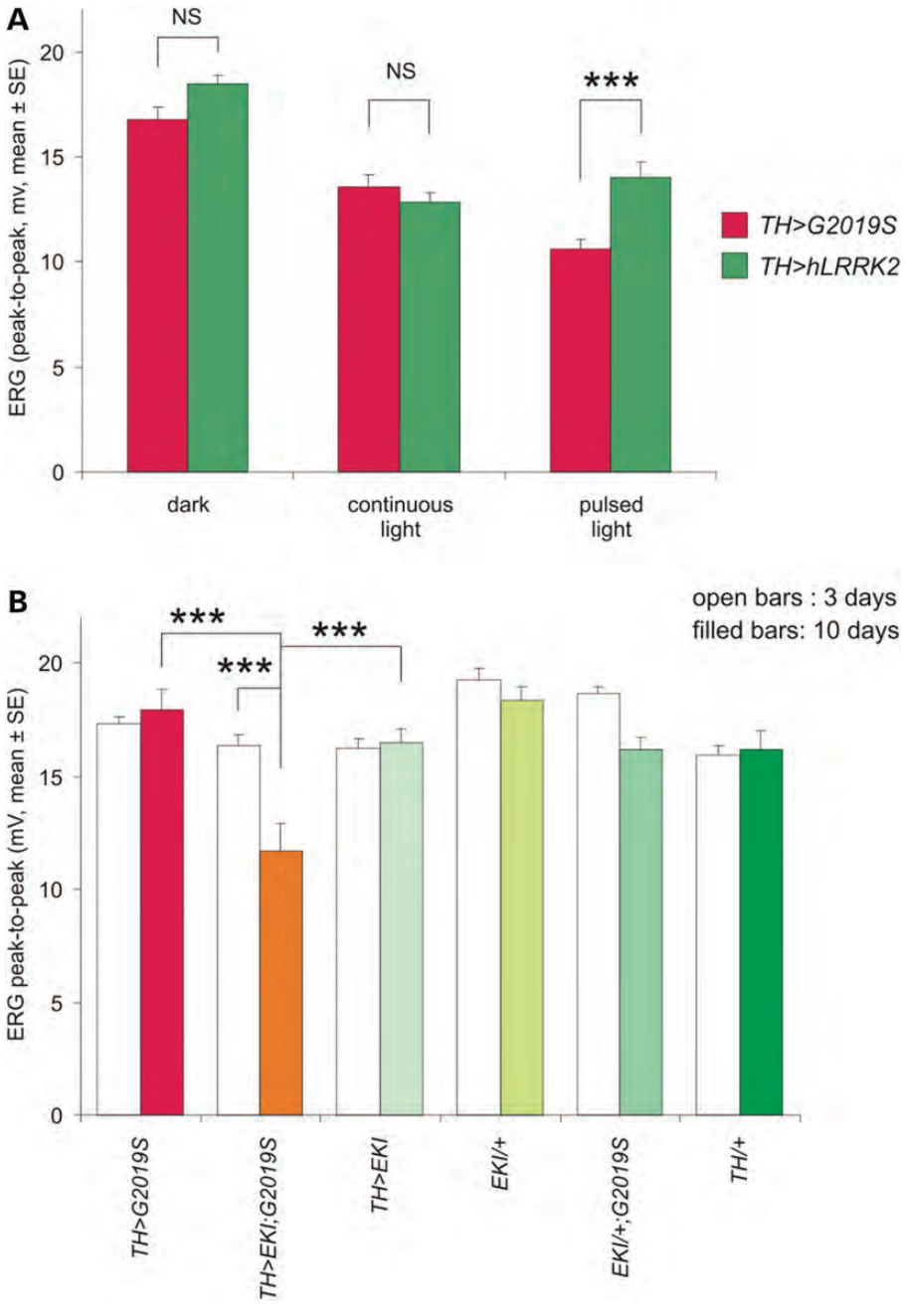

Figure 9. *G2019S*-induced degeneration is enhanced by neuronal activity. (**A**) Flies were kept for 10 days in constant dark, constant blue illumination or with the blue light turned on–off at randomized intervals (mean ~1.5 s). Comparison of *TH > G2019S* and *TH > hLRRK2* only shows a difference in pulsed light, when the *TH > G2019S* showed reduced electroretinogram (ERG) amplitude (Bonferroni *post-hoc* test, $P = 0.001$). The pulsed light *G2019S* flies also had reduced ERGs compared with those in constant light ($P = 0.006$), but there is no significant difference between *hLRRK2* flies in constant and pulsed illumination. (**B**) Reducing the activity of potassium channels in the dopaminergic neurons accelerates the loss of visual function seen with *G2019S*. When *TH* GAL4 was used to express both the *LRRK2-G2019S* mutation and the *EKI* transgene (a combination of dominant negative forms of the *shaker* (*sh*) and *ether a go-go* (*eag*) potassium channels), a loss of visual function is already seen at 10 days (red bar, $P < 0.001$), whereas all the other genotypes shown have a normal visual response (comparison of the *TH > G2019S*;*EKI* with any other sample, $P = < 0.001$). Using *TH* to express the *EKI* transgene alone had no impact on visual function. Data in (A) from 60 flies kept at 29°C, in (B) from 122 flies kept in the dark in the 29°C incubator; for details of the number of flies see Supplementary Material, Table S1.

dopaminergic neurons, retinal surface abnormalities and neurodegeneration (reviewed in 41). This has been ascribed to differences in microscopical technique (19,41) or food (42,43). Our data suggest another explanation: the level of neuronal demands for energy is important in the PD models. This leads to the idea that increasing the activity of the visual system in mouse models of PD may provide a more consistent phenotype. Finally, we suggest that the selective death of some

dopaminergic neurons and survival of others, both in flies (26,44) and mammals (45,46), could be due to differences in neuronal activity.

MATERIALS AND METHODS

Flies

Stock vials of *Drosophila melanogaster* were raised on yeast–sucrose–agar fly food. Directed expression of *LRRK2*-related transgenes was achieved using the GAL4/ UAS system, with lines described as follows: UAS-*hLRRK2* and UAS-*G2019S* (14), UAS-*dLRRK* and UAS-*dLRRK-3KD* (*dLRRK-K1781M-D1882A-D1912A*) (47), UAS-*dLRRK I1915T* and UAS-*dLRRK Y1383C* (25), UAS-*I2020T* and UAS-*I1122V* (18), UAS-*G2019S-K1906M*, UAS-*G2385R* and UAS-*R1441C* (13), *HL9* GAL4 (48), *L1L2B* GAL4 (15), *dLRRK* (e03680) (49); and using lines from Matthias Landgraf (UAS-*myr-GFP*), Stephen Goodwin (*TH* and *nSyb* GAL4) and Manolis Fanto (UAS-*ATG5* and UAS-*ATG5-RNAi*); from Bloomington (UAS- *eIf-4A3-GFP*) or from laboratory stocks (*Actin5c, LongGMR* and $elav^{3e1}$ GAL4 lines and the w^{1118} (+) and *Canton-S* (*CS*) wild-types). The EKI transgene is a combined UAS-$shaker^{DN}$ *-ether a go-go*^{DN} construct (20,21). In Figure 2, we also tested the UAS-*hLRRK2* and UAS-*G2019S* lines from Lin *et al*. (13) (marked with *) and found their ERGs resembled those of Liu *et al*. (14) (marked with †).

Experimental crosses were raised on maize-meal fly food at 25°C. On the day of emergence, females were transferred to vials of yeast–sucrose–agar fly food in a dark incubator at 29°C. Flies were moved to fresh vials every 3 or 4 days, and so were exposed to light occasionally. In pulsating light experiments, vials were placed in an opaque plastic tube, stoppered with cotton wool in the 29°C incubator. The side wall of the tube contained high-intensity tricolour light-emitting diodes (LEDs, Kingbright, KAF-5060PBESEEVGC, maximum blue emission wavelength 465 nm). These were either off, on or randomly toggled on/off under computer control. Only the blue component was ever turned on.

ERGs were by aspirating (unanaesthetized) females into shortened pipette tips and restraining them using nail varnish (Creative Nail Design). Recordings were made between blunt glass pipette electrodes, filled with simple *Drosophila* saline (130 mM NaCl, 4.7 mM KCl, 1.9 mM $CaCl_2$) (50). The recording electrode was placed in the centre of the eye with a reference electrode in the mouthparts. Three to five stimuli (10 s apart, 0.5 s long) were presented after 2 min adaptation in the dark laboratory, from the blue component of LEDs, (Kingbright, KAF-5060PBESEEVGC, maximum emission wavelength 465 nm) placed ~6 cm in front of the fly. Stimuli were monitored with a BPX65 photodiode (Centronics) placed next to the pipette tip. The photodiode current was 0.5 nA in the darkened laboratory and 400 nA during the stimuli. Each genotype/timepoint sample is the average (±SE) from at least seven flies.

Anatomy

Head sections were made as described recently (51). Heads were fixed (4% paraformaldehyde, 1% glutaraldehyde in 0.1 M sodium phosphate buffer, pH 7.4), followed by 1% osmium tetroxide, dehydrated through an acetone series, followed by infiltration and embedding in Spurr's resin. Semi-thick serial sections (1.0 μm; Leica Ultracut UCT) were stained with 0.6% toluidine blue in 0.3% sodium carbonate and imaged with a Zeiss Axiovert 200 microscope and Zeiss AxioCam HRm camera. Thin sections were cut and stained with uranyl acetate and Reynolds lead citrate. Images were captured with an Olympus-SIS Megaview III camera using analySIS software on a Tecnai 12 BioTWIN G2 (software version 2.1.8) operating at 120 kV. Tangential sections taken at the level of the outer part of the microvilli were analysed. The area of the mitochondria was measured from high-power images (samples in Fig. 6Aii) using ImageJ. The width of the cristae was estimated by counting the number of cristae which crossed a line drawn on the long axis of the mitochondria.

Confocal images

These were acquired from brains (including the optic lobes), dissected from *TH > GFP* expressing flies, fixed in 4% paraformaldehyde for 30 min. This and all subsequent incubations were performed at room temperature. After permeabilization in 0.5% Triton X-100 for 30 min, the brains were incubated in mouse anti-TH (Immunostar, 1:1000) together with rabbit anti-GFP (Abcam, 1:1000) for 3 h. After washing, the brains were transferred to a solution containing Cy3 conjugated goat anti-mouse IgG (Abcam, 1:250) and FITC conjugated goat anti-rabbit IgG (Abcam, 1:250) for a further 3 h. After further washing, the brains were mounted in Vectashield (Vector Laboratories). Eyes were dissected and fixed in 3.7% formaldehyde, and stained with ATG5 (Anti-Rabbit ATG5, Novus Biological 1:300 dilution) or cleaved caspase 3 antibody (anti-Rabbit Cleaved caspase-3 (Asp175), Cell Signaling Technology, 1:1600 dilution), which recognizes the effector caspases DRICE and DCP-1 in *Drosophila* (52,53). Confocal images were obtained using a Zeiss 780 microscope. The external surface of the eyes of etherized females was photographed using a Zeiss Stemi microscope and ERc 5 s camera.

Detection of protein expression in *Drosophila* lysates

FLAG-LRRK2

For each genotype, 30 fly heads were dissected and immediately homogenized on ice in 30 μl 2X SDS sample buffer (Sigma), boiled for 10 min and then separated by SDS–PAGE on a 7.5% polyacrylamide gel. The proteins were transferred to a PVDF membrane by electrophoresis and probed with mouse anti-FLAG (1:1000; M2 clone, Sigma) and a goat anti-mouse-HRP secondary antibody (1:5000; Sigma), followed by visualization with enhanced chemiluminescence (Millipore). To control for equal protein loading, the membrane was re-probed with mouse anti-β-actin (1:10 000; Proteintech) or rabbit anti-Synaptotagmin antibody, used at 1:1000.

Cleaved caspase 3

Eyes (40) were dissected on dry ice, lysed in sample buffer (10 μg/ml) and boiled for 5 min, before resolving on 12%

SDS polyacrylamide gels. Blots were probed with anti-cleaved caspase 3 (ASP175) (1:1000, Cell Signalling Technology) and developed using HRP conjugated anti-rabbit and enhanced chemiluminescence. In order to test for equal loading of the proteins, the membrane was stripped and re-probed with mouse anti-β-actin (1:1000 Ambion).

SUPPLEMENTARY MATERIAL

Supplementary Material is available at *HMG* online.

ACKNOWLEDGEMENTS

We are grateful to those who sent gifts of flies: Wanli Smith, Bingwei Lu, Yuzuru Imai, Cheng-Ting Chien, Katerina Venderova, Zhuohua Zhang, Matthias Landgraf, Subhabrata Sanyal, Stephen Goodwin, Manolis Fanto, Gero Miesenboeck, Charlotte Foerster and Jens Rister. We would like to thank Ryan West, Shaun Calvert and Rebecca Furmston for assistance with data collection. John Sparrow and Alex Wade kindly commented on the manuscript.

Conflict of Interest statement. None declared.

FUNDING

We were supported by Parkinson's UK (grant number K-1007), the Wellcome Trust (grant number 097829/Z/11/A) and Biotechnology and Biological Sciences Research Council. Funding to pay the Open Access publication charges for this article was provided by The Wellcome Trust.

REFERENCES

1. Archibald, N.K., Clarke, M.P., Mosimann, U.P. and Burn, D.J. (2009) The retina in Parkinson's disease. *Brain*, **132**, 1128–1145.
2. Crooks, J. and Kolb, H. (1992) Localization of GABA, glycine, glutamate and tyrosine hydroxylase in the human retina. *J. Comp. Neurol.*, **315**, 287–302.
3. Witkovsky, P. (2004) Dopamine and retinal function. *Doc. Ophthal.*, **108**, 17–39.
4. Ribelayga, C., Cao, Y. and Mangel, S.C. (2008) The circadian clock in the retina controls rod-cone coupling. *Neuron*, **59**, 790–801.
5. Harnois, C. and Di Paolo, T. (1990) Decreased dopamine in the retinas of patients with Parkinson's disease. *Invest. Opthal. Vis. Sci.*, **31**, 2473.
6. Devos, D., Tir, M., Maurage, C.A., Waucquier, N., Defebvre, L., Defoort-Dhellemmes, S. and Destee, A. (2005) ERG and anatomical abnormalities suggesting retinopathy in dementia with Lewy bodies. *Neurol.*, **65**, 1107–1110.
7. Nassel, D.R., Elekes, K. and Johansson, K.U. (1988) Dopamine-immunoreactive neurons in the blowfly visual system: light and electron microscopic immunocytochemistry. *J. Chem. Neuroanat.*, **1**, 311.
8. Hamasaka, Y. and Nassel, D.R. (2006) Mapping of serotonin, dopamine, and histamine in relation to different clock neurons in the brain of Drosophila. *J. Comp. Neurol.*, **494**, 314–330.
9. Sanes, J.R. and Zipursky, S.L. (2010) Design principles of insect and vertebrate visual systems. *Neuron*, **66**, 15.
10. Chyb, S., Hevers, W., Forte, M., Wolfgang, W.J., Selinger, Z. and Hardie, R.C. (1999) Modulation of the light response by cAMP in Drosophila photoreceptors. *J. Neurosci.*, **19**, 8799–8807.
11. Zimmerman, J.E., Naidoo, N., Raizen, D.M. and Pack, A.I. (2008) Conservation of sleep: insights from non-mammalian model systems. *Trends Neurosci.*, **31**, 371–376.
12. Hirsh, J., Riemensperger, T., Coulom, H., Iche, M., Coupar, J. and Birman, S. (2010) Roles of dopamine in circadian rhythmicity and extreme light sensitivity of circadian entrainment. *Curr. Biol.*, **20**, 209–214.
13. Lin, C.H., Tsai, P.I., Wu, R.M. and Chien, C.T. (2010) LRRK2 G2019S mutation induces dendrite degeneration through mislocalization and phosphorylation of tau by recruiting autoactivated GSK3+¦. *J. Neurosci.*, **30**, 13138–13149.
14. Liu, Z., Wang, X., Yu, Y., Li, X., Wang, T., Jiang, H., Ren, Q., Jiao, Y., Sawa, A., Moran, T. *et al.* (2008) A Drosophila model for LRRK2-linked parkinsonism. *Proc. Natl Acad. Sci. USA*, **105**, 2693–2698.
15. Rister, J., Pauls, D., Schnell, B., Ting, C.Y., Lee, C.H., Sinakevitch, I., Morante, J., Strausfeld, N.J., Ito, K. and Heisenberg, M. (2007) Dissection of the peripheral motion channel in the visual system of Drosophila melanogaster. *Neuron*, **56**, 155–170.
16. Cookson, M.R. and Bandmann, O. (2010) Parkinson's disease: insights from pathways. *Hum. Mol. Genet.*, **19**, R21–R27.
17. Moore, D.J. (2008) The biology and pathobiology of LRRK2: implications for Parkinson's disease. *Park. Rel. Disorder*, **14**, S92–S98.
18. Venderova, K., Kabbach, G., Bdel-Messih, E., Zhang, Y., Parks, R.J., Imai, Y., Gehrke, S., Ngsee, J., LaVoie, M.J. and Slack, R. (2009) Leucine-rich repeat kinase interacts with Parkin, DJ-1 and PINK-1 in a Drosophila melanogaster model of Parkinson's disease. *Hum. Mol. Genet.*, **18**, 4390–4404.
19. Drobysheva, D., Ameel, K., Welch, B., Ellison, E., Chaichana, K., Hoang, B., Sharma, S., Neckameyer, W., Srinakevitch, I. and Murphy, K.J. (2008) An optimized method for histological detection of dopaminergic neurons in Drosophila melanogaster. *J. Histochem. Cytochem.*, **56**, 1049–1063.
20. Duch, C., Vonhoff, F. and Ryglewski, S. (2008) Dendrite elongation and dendritic branching are affected separately by different forms of intrinsic motoneuron excitability. *J. Neurophysiol.*, **100**, 2525–2536.
21. Hartwig, C.L., Worrell, J., Levine, R.B., Ramaswami, M. and Sanyal, S. (2008) Normal dendrite growth in Drosophila motor neurons requires the AP-1 transcription factor. *Dev. Neurobiol.*, **68**, 1225–1242.
22. Greggio, E. and Cookson, M.R. (2009) Leucine-rich repeat kinase 2 mutations and Parkinson's disease: three questions. *ASN Neuro*, **1**, e00002.
23. Feany, M.B. and Bender, W.W. (2000) A Drosophila model of Parkinson's disease. *Nature*, **404**, 394–398.
24. Chen, L. and Feany, M.B. (2005) Alpha-synuclein phosphorylation controls neurotoxicity and inclusion formation in a Drosophila model of Parkinson disease. *Nat. Neurosci.*, **8**, 657–663.
25. Imai, Y., Gehrke, S., Wang, H.Q., Takahashi, R., Hasegawa, K., Oota, E. and Lu, B. (2008) Phosphorylation of 4E-BP by LRRK2 affects the maintenance of dopaminergic neurons in Drosophila. *EMBO J.*, **27**, 2432–2443.
26. Ng, C.H., Mok, S.Z.S., Koh, C., Ouyang, X., Fivaz, M.L., Tan, E.K., Dawson, V.L., Dawson, T.M., Yu, F. and Lim, K.L. (2009) Parkin protects against LRRK2 G2019S mutant-induced dopaminergic neurodegeneration in Drosophila. *J. Neurosci.*, **29**, 11257–11262.
27. Ng, C.H., Guan, M.S.H., Koh, C., Ouyang, X., Yu, F., Tan, E.K., O'Neill, S.P., Zhang, X., Chung, J. and Lim, K.L. (2012) AMP kinase activation mitigates dopaminergic dysfunction and mitochondrial abnormalities in Drosophila models of Parkinson's disease. *J. Neurosci.*, **32**, 14311–14317.
28. Mortiboys, H., Johansen, K.K., Aasly, J.O. and Bandmann, O. (2010) Mitochondrial impairment in patients with Parkinson disease with the G2019S mutation in LRRK2. *Neurology*, **75**, 2017–2020.
29. MacLeod, D., Dowman, J., Hammond, R., Leete, T., Inoue, K. and Abeliovich, A. (2006) The familial parkinsonism gene *LRRK2* regulates neurite process morphology. *Neuron*, **52**, 587–593.
30. Gao, S., Takemura, S.Y., Ting, C.Y., Huang, S., Lu, Z., Luan, H., Rister, J., Thum, A.S., Yang, M., Hong, S.T. *et al.* (2008) The neural substrate of spectral preference in Drosophila. *Neuron*, **60**, 328–342.
31. Li, X., Patel, J.C., Wang, J., Avshalumov, M.V., Nicholson, C., Buxbaum, J.D., Elder, G.A., Rice, M.E. and Yue, Z. (2010) Enhanced striatal dopamine transmission and motor performance with LRRK2 overexpression in mice is eliminated by familial Parkinson's disease mutation G2019S. *J. Neurosci.*, **30**, 1788–1797.
32. Taylor, J.P., Hardy, J. and Fischbeck, K.H. (2002) Toxic proteins in neurodegenerative disease. *Science*, **296**, 1991–1995.
33. Attwell, D. and Laughlin, S.B. (2001) An energy budget for signaling in the grey matter of the brain. *J. Cereb. Blood Flow Metab.*, **21**, 1133–1145.

34. Laughlin, S.B., van Steveninck, R.R.R. and Anderson, J.C. (1998) The metabolic cost of neural information. *Nat. Neurosci.*, **1**, 36–41.
35. Raghu, P., Usher, K., Jonas, S., Chyb, S., Polyanovsky, A. and Hardie, R.C. (2000) Constitutive activity of the light-sensitive channels TRP and TRPL in the Drosophila diacylglycerol kinase mutant, rdgA. *Neuron*, **26**, 169–179.
36. Geng, C., Pellegrino, A., Bowman, J., Zhu, L. and Pak, W.L. (2004) Complete RNAi rescue of neuronal degeneration in a constitutively active Drosophila TRP channel mutant. *BBA - General Subjects*, **1674**, 91–97.
37. Mast, J.D., Tomalty, K.M.H., Vogel, H. and Clandinin, T.R. (2008) Reactive oxygen species act remotely to cause synapse loss in a Drosophila model of developmental mitochondrial encephalopathy. *Devel.*, **135**, 2669–2679.
38. Vincent, A., Briggs, L., Chatwin, G.F.J., Emery, E., Tomlins, R., Oswald, M., Middleton, C.A., Evans, G.J.O., Sweeney, S.T. and Elliott, C.J.H. (2012) *Parkin* induced defects in neurophysiology and locomotion are generated by metabolic dysfunction and not oxidative stress. *Hum. Mol. Genet.*, **21**, 1760–1769.
39. Bishop, M.W., Chakraborty, S., Matthews, G.A.C., Dougalis, A., Wood, N.W., Festenstein, R. and Ungless, M.A. (2010) Hyperexcitable substantia nigra dopamine neurons in PINK1- and HtrA2/Omi-deficient mice. *J. Neurophysiol.*, **104**, 3009–3020.
40. Guzman, J.N., Sanchez-Padilla, J., Wokosin, D., Kondapalli, J., Ilijic, E., Schumacker, P.T. and Surmeier, D.J. (2010) Oxidant stress evoked by pacemaking in dopaminergic neurons is attenuated by DJ-1. *Nature*, **468**, 696–700.
41. Whitworth, A.J. (2011) Drosophila models of Parkinson's disease. *Adv. Genet.*, **73**, 1–50.
42. Saini, N. and Schaffner, W. (2010) Zinc supplement greatly improves the condition of parkin mutant Drosophila. *Biol. Chem.*, **391**, 513–518.
43. Saini, N., Oelhafen, S., Hua, H., Georgiev, O., Schaffner, W. and Bueler, H. (2010) Extended lifespan of Drosophila parkin mutants through sequestration of redox-active metals enhancement of anti-oxidative pathways. *Neurobiol. Dis.*, **40**, 82–92.
44. Whitworth, A.J., Theodore, D.A., Greene, J.C., Benes, H., Wes, P.D. and Pallanck, L.J. (2005) Increased glutathione S-transferase activity rescues dopaminergic neuron loss in a Drosophila model of Parkinson's disease. *Proc. Natl Acad. Sci. USA*, **102**, 8024–8029.
45. Kish, S.J., Shannak, K. and Hornykiewicz, O. (1988) Uneven pattern of dopamine loss in the striatum of patients with idiopathic Parkinson's disease. *N. Engl. J. Med.*, **318**, 876–880.
46. Damier, P., Hirsch, E.C., Agid, Y. and Graybiel, A.M. (1999) The substantia nigra of the human brain. *Brain*, **122**, 1437–1448.
47. Lee, S., Liu, H.P., Lin, W.Y., Guo, H. and Lu, B. (2010) LRRK2 kinase regulates synaptic morphology through distinct substrates at the presynaptic and postsynaptic compartments of the Drosophila neuromuscular junction. *J. Neurosci.*, **30**, 16959–16969.
48. Claridge-Chang, A., Roorda, R.D., Vrontou, E., Sjulson, L., Li, H., Hirsh, J. and Miesenboeck, G. (2009) Writing memories with light-addressable reinforcement circuitry. *Cell*, **139**, 405–415.
49. Wang, D., Tang, B., Zhao, G., Pan, Q., Xia, K., Bodmer, R. and Zhang, Z. (2008) Dispensable role of Drosophila ortholog of LRRK2 kinase activity in survival of dopaminergic neurons. *Mol. Neurodegener.*, **3**, 3.
50. Heisenberg, M. (1971) Separation of receptor and lamina potentials in the electroretinogram of normal and mutant Drosophila. *J. Exp. Biol.*, **55**, 85.
51. Hindle, S.J. (2010) Modelling saposin deficiency in Drosophila: progressive neurodegeneration, storage and physiological decline. PhD Thesis, University of York.
52. Yan, N., Huh, J.R., Schirf, V., Demeler, B., Hay, B.A. and Shi, Y. (2006) Structure and activation mechanism of the Drosophila initiator caspase Dronc. *J. Biol. Chem.*, **281**, 8667–8674.
53. Fan, Y. and Bergmann, A. (2009) The cleaved-Caspase-3 antibody is a marker of Caspase-9-like DRONC activity in Drosophila. *Cell Death Diff.*, **17**, 534–539.
54. Kumari, U. and Tan, E.K. (2009) LRRK2 in Parkinson's disease: genetic and clinical studies from patients. *FEBS J.*, **276**, 6455–6463.